



Molecular Crystals and Liquid Crystals

Publication details, including instructions for authors and subscription information:

<http://www.tandfonline.com/loi/gmcl20>

Photovoltaic Properties of N-Pyrrolidinyl Substituted Perylenebis(dicarboximide) Derivatives

Won Suk Shin^a, Hwan-Hee Jung^a, Mi-Kyoung Kim^a, Mi-Ra Kim^a, Mi-Kyoung Kim^a, B. Vijaya Kumar Naidu^a, Sung-Ho Jin^a, Jin-Kook Lee^b, Jae Wook Lee^c & Yeong-Soon Gal^d

^a Department of Chemistry Education and Center for Plastic Information System, Pusan National University, Busan, Korea

^b Department of Polymer Science and Engineering, Pusan National University, Busan, Korea

^c Department of Chemistry, Dong-A University, Busan, Korea

^d Polymer Chemistry Lab., Kyungil University, Hayang, Korea

Version of record first published: 17 Oct 2011

To cite this article: Won Suk Shin, Hwan-Hee Jung, Mi-Kyoung Kim, Mi-Ra Kim, Mi-Kyoung Kim, B. Vijaya Kumar Naidu, Sung-Ho Jin, Jin-Kook Lee, Jae Wook Lee & Yeong-Soon Gal (2006): Photovoltaic Properties of N-Pyrrolidinyl Substituted Perylenebis(dicarboximide) Derivatives, *Molecular Crystals and Liquid Crystals*, 462:1, 59-66

To link to this article: <http://dx.doi.org/10.1080/15421400601009401>

PLEASE SCROLL DOWN FOR ARTICLE

Full terms and conditions of use: <http://www.tandfonline.com/page/terms-and-conditions>

This article may be used for research, teaching, and private study purposes. Any substantial or systematic reproduction, redistribution, reselling, loan, sub-licensing, systematic supply, or distribution in any form to anyone is expressly forbidden.

The publisher does not give any warranty express or implied or make any representation that the contents will be complete or accurate or up to date. The accuracy of any instructions, formulae, and drug doses should be independently verified with primary sources. The publisher shall not be liable for any loss, actions, claims, proceedings, demand, or costs or damages whatsoever or howsoever caused arising directly or indirectly in connection with or arising out of the use of this material.

Photovoltaic Properties of N-Pyrrolidinyl Substituted Perylenebis(dicarboximide) Derivatives

Won Suk Shin

Hwan-Hee Jung

Mi-Kyoung Kim

Mi-Ra Kim

Mi-Kyoung Kim

B. Vijaya Kumar Naidu

Sung-Ho Jin

Department of Chemistry Education and Center for Plastic Information System, Pusan National University, Busan, Korea

Jin-Kook Lee

Department of Polymer Science and Engineering, Pusan National University, Busan, Korea

Jae Wook Lee

Department of Chemistry, Dong-A University, Busan, Korea

Yeong-Soon Gal

Polymer Chemistry Lab., Kyungil University, Hayang, Korea

N,N'-Di(1-nonadecyl)perylene-3,4:9,10-bis(dicarboximide) (PDI-C9) based bulk-heterojunction photovoltaic devices increased the power conversion efficiency (PCE) with increasing PDI-C9 concentration and showed the highest incident photon-to-current conversion efficiency (IPCE) of 19% at 495 nm and PCE of 0.18% under AM 1.5 (100 mW/cm²) have been achieved with 1:4 ratio of P3HT: PDI-C9. 1,7-Bis(N-pyrrolidinyl)-N,N'-dicyclohexyl-3,4:9,10-perylenebis(dicarboximide) (5-PDI-DI) based devices showed best performance of 9% IPCE at 525 nm

This work was supported by the Ministry of Information & Communications, Korea, under the Information Technology Research Center (ITRC) Support Program.

Address correspondence to Sung-Ho Jin, Department of Chemistry Education and Center for Plastic Information System, Pusan National University, Busan 609-735, Korea. E-mail: shjin@pusan.ac.kr

and 0.18% (AM 1.5) PCE at 1:1 blend ratio of P3HT: 5-PDI-DI and the PCEs were drastically decreased by increasing 5-PDI-DI ratio.

Keywords: annealing; heterojunction; perylene diimide; photovoltaic

INTRODUCTION

Organic materials for photovoltaic devices based on conducting polymers are attractive because most of them can be processed from solution via spin-coating at room temperature, enabling the manufacture of large area, flexible, and lightweight devices. Current progress on organic photovoltaic devices from the standpoint of increasing power conversion efficiency (PCE) is mainly attributed to the bulk heterojunction structure, which enables an efficient charge separation due to the increased photoactive interface area of p-n junction. The highest efficiency of 3.5% have been reported so far, and recently 5% efficiency benchmark has been overcome [1]. But, further increase of the PCE is required for commercial applications of organic photovoltaic solar cells.

In order to increase the PCE of devices, many aspects should be taken into account, such as the absorption coefficients of the materials, the exciton dissociation rates and the charge-carrier mobilities. First of all, the active layer should absorb as many as incident photons to generate excitons. Most of the electron acceptors such as C₆₀ derivatives and TiO₂ nanoparticles for the bulk heterojunction photovoltaic devices are having relatively weak molar absorption coefficients at the visible region and do not give any direction for self-assembly when they were blended with electron donor polymers. We are interested in perylene diimide derivatives (**PDI**s), because **PDI**s have large molar absorption coefficients, good electron accepting properties [2] and possible generation of highly conducting direction along the π - π stacking axis [3,4], in addition to the other merits, like robust, thermally stable, and inexpensive. Up to date, most of the applications for photovoltaic devices with perylene derivatives were performed to dye-sensitized solar cell (DSSC) [5] or layered structure through vapor deposition with insoluble **PDI**s [6], but the applications of the **PDI**s to the bulk heterojunction photovoltaic devices are quite limited [7].

Thus, in this paper we investigated three different **PDI**s: N,N'-di(1-nonadecyl)perylene-3,4:9,10-bis(dicarboximide) (**PDI-C9**), 1-(N-pyrrolidinyl)-N,N'-dicyclohexyl-3,4:9,10-perylenebis(dicarboximide) (**5-PDI-MONO**), 1,7-bis(N-pyrrolidinyl)-N,N'-dicyclohexyl-3,4:9,10-perylenebis(dicarboximide) (**5-PDI-DI**). **PDI-C9** has swallow tailed

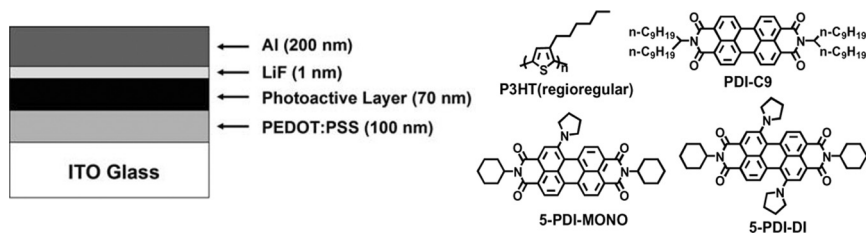


FIGURE 1 Device configuration and the chemical structures of **P3HT** and perylene diimide derivatives (**PDIs**).

long alkyl chains to give good solubility. Introduction of pyrrolidinyl group at the bay position of perylene shifted the absorption region to longer wavelength [8] and changed the LUMO levels of **5-PDI-MONO** and **5-PDI-DI** by its electron donating effect. The conjugated polymer poly(3-hexylthiophene) (**P3HT**), which is known to be a good hole mobility molecule in its regioregular form [9], has been chosen as a electron donor as well as a hole conductor. The device configuration and compound structures are shown in Figure 1.

EXPERIMENTAL

Synthesis and Preparation of Materials

Regioregular **P3HT** purchased from Aldrich and the poly(ethylene-dioxythiophene) doped with poly(styrenesulfonic acid) (PEDOT:PSS, Baytron[®] PH) purchased from Baytron were used without further purification. 3,4,9,10-Perylenetetracarboxylic dianhydride was supplied by Phthalos (South Korea). The **PDI-C9** [10], **5-PDI-MONO** and **5-PDI-DI** [8] were synthesized and purified by literature methods.

Photovoltaic Device Fabrication

Films of different weight ratios of the **P3HT** and **PDIs** were spin coated from o-dichlorobenzene solution onto indium tin oxide (ITO) covered glass substrates that had been previously coated with 100 nm of PEDOT:PSS. Then, LiF (1 nm) and Al top electrode (200 nm) were deposited by means of thermal evaporation in vacuo (base pressure $< 2.0 \times 10^{-6}$ torr) onto the organic layer through a shadow mask. The pixel size as defined by the overlap with ITO and Al back electrode was 4 mm^2 . Thermal treatment was performed under dry Ar atmosphere on a high precision hot stage. The current-voltage

curve of the photovoltaic device was measured under the illumination of a simulated solar light with 100 mW/cm^2 (AM1.5) by an Oriel 300 W solar simulator. The photocurrent action spectra were carried out by illuminating the samples with a 300 W Xenon lamp, dispersed by Dongwoo-optron (South Korea) DM151i single-grating monochromator. Film thickness was measured using a KLA Tencor Alpha-step IQ surface profilometer.

RESULTS AND DISCUSSION

From the UV-visible spectroscopic results of **PDI**s presented in Figure 2, the maximum absorption peaks of **PDI-C9** and **5-PDI-MONO** in solid film had hypsochromic shift when they solidified during spin cast from chloroform solution. This blue shift was caused by the H-aggregation of perylene moiety, which means **PDI**s were aggregated via face to face self-assembly [3]. The extended H-aggregation in the donor polymer in the blend device could give the charge transporting channel along the π - π stacking axis [3,4]. However, in the case of **5-PDI-DI**, the maximum absorption peak was not moved except the short wavelength shoulder increasing. This means that two pyrrolidinyl groups in **5-PDI-DI** restrict its face to face self-assembly. By introducing pyrrolidinyl group on **PDI** one by one, the absorption spectra were drastically shifted to longer wavelength region. In film state, the absorption maximum of **5-PDI-MONO** and **5-PDI-DI** had bathochromic shifts 105 nm and 201 nm respectively from **PDI-C9**. This long visible light absorption property of **5-PDI-MONO** and **5-PDI-DI** could be a good advantage to use the whole range of the visible light by fabricating photovoltaic device after blending with **P3HT**.

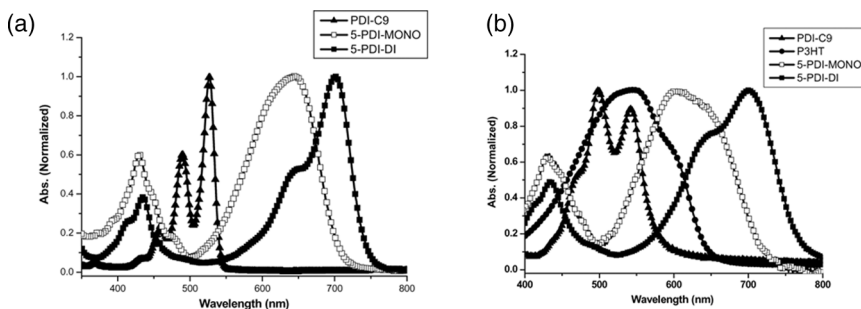


FIGURE 2 UV-visible spectra of; a) **PDI**s in chloroform solution, b) **PDI**s and **P3HT** spin-coated on quartz from chloroform solution.

The LUMO energy levels of **PDI-C9** (3.69 eV), **5-PDI-MONO** (3.46 eV) and **5-PDI-DI** (3.40 eV) were obtained from the half way reduction potentials ($E_{1/2}^{-1}$) and the HOMO levels of **PDI-C9** (5.97 eV), **5-PDI-MONO** (5.18 eV) and **5-PDI-DI** (5.00 eV) were estimated by the addition of the optical band gap from the LUMO levels. The HOMO (5.20 eV) and LUMO (3.34 eV) energy levels of **P3HT** were obtained from the onset potential of the oxidation at CV and the optical band gap. The optical band gaps were determined by the absorption edge of their thin films. **PDI-C9** has the proper HOMO and LUMO levels to accept the electron from the excited **P3HT** molecule and to transfer the hole from the excited **PDI-C9** to **P3HT**. But for **5-PDI-MONO** and **5-PDI-DI**, HOMO levels were slightly higher than the HOMO level of **P3HT** and it could have some possibility to render the undesired energy transfer from **P3HT** to **5-PDI-MONO** and **5-PDI-DI** rather than charge separation.

Table 1 summarizes photovoltaic device performance results. The annealing were performed at higher temperature than their grass transition temperature ($T_g^{\text{PDI-C9}} = 76^\circ\text{C}$, $T_g^{\text{5-PDI-MONO}} = 109^\circ\text{C}$ and $T_g^{\text{5-PDI-DI}} = 105^\circ\text{C}$). PCE of the most devices were increased with

TABLE 1 Performance of ITO/PEDOT:PSS/P3HT:PDIs/LiF/Al Bulk Heterojunction Photovoltaic Devices Under a Simulated Photovoltaic Light with 100 mW/cm² Illumination with 70 nm Active Layer Thickness

PDIs	Device	P3HT/PDI ratio	Annealing	J_{sc} [mA/cm ²]	V_{oc} [V]	FF	PCE [%]
PDI-C9	a	1/1	–	0.47	0.23	0.31	0.034
	b	1/1	80°C, 60 min	0.67	0.29	0.33	0.065
	c	1/2	–	0.73	0.27	0.35	0.068
	d	1/2	80°C, 60 min	1.09	0.25	0.37	0.100
	e	1/4	–	1.31	0.30	0.38	0.139
	f	1/4	80°C, 60 min	1.32	0.36	0.38	0.182
5-PDI-MONO	g	1/1	–	0.65	0.48	0.28	0.085
	h	1/1	110°C, 30 min	0.73	0.51	0.29	0.107
	i	1/2	–	0.16	0.54	0.26	0.023
	j	1/2	110°C, 30 min	0.19	0.49	0.27	0.026
	k	1/4	–	0.11	0.46	0.27	0.014
	l	1/4	110°C, 30 min	0.12	0.45	0.28	0.015
5-PDI-DI	m	1/1	–	0.75	0.54	0.35	0.142
	n	1/1	110°C, 30 min	0.90	0.62	0.32	0.180
	o	1/2	–	0.23	0.56	0.27	0.035
	p	1/2	110°C, 30 min	0.18	0.59	0.28	0.030
	q	1/4	–	0.05	0.40	0.25	0.005
	r	1/4	110°C, 30 min	0.03	0.31	0.22	0.002

annealing. The increased device performance may be due to the reorientation of **P3HT** [7] and **PDIs** to get more ordered stacking during annealing. With increasing **PDI-C9** ratio in **P3HT:PDI-C9** blend system, the PCE also increased gradually and reached to a maximum of 0.182% at 1:4 ratio (**device f**). On the other hand, **5-PDI-MONO** and **5-PDI-DI** based devices show best performance of 0.107% and 0.180% at 1:1 blend ratio and which is much better than that of **PDI-C9** based device at the 1:1 ratio of **P3HT:PDI-C9**. But the PCE were drastically decreased by adding more **5-PDI-MONO** and **5-PDI-DI**. The increase of the performance with the concentration of **PDI-C9** may due to the generation of percolation paths for electrons by increasing more small crystals or self-assembled structure portions [7a]. In the case of **5-PDI-MONO** and **5-PDI-DI**, which have more uniformly spread over the device because of their solubility increasing pyrrolidinyl side groups, the electrons could more easily reached the cathode by transferring through pyrrolidinyl groups in addition to face to face self-assembled pathway from perylene to perylene. Pyrrolidinyl side groups give the good solubility but inhibit the well stacking of **5-PDI-MONO** and **5-PDI-DI** and their good miscibility with **P3HT** inhibits the ordered structure of **P3HT**, which resulted in the limited charge transporting ability in **P3HT** at high concentration of **5-PDI-MONO** and **5-PDI-DI**.

When electron donating group is fixed with **P3HT**, the V_{OC} is attributed to the LUMO level of the **PDIs**, so the introduction of electron donating group at the perylene body could increase the V_{OC} by increasing LUMO level. Actually the increase of LUMO level by 0.3 V with introducing electron donating pyrrolidinyl group renders the increase of V_{OC} nearly 0.3 V at **5-PDI-DI** ($V_{OC} = \sim 0.6$ V). This is quite well matched with the variation of the valence band of n-type semiconductor resulting in a change of the open circuit voltage with a scaling factor of ~ 1 [1b].

Incident photon-to-current conversion efficiency (IPCE) of the device made with **PDI-C9** (**device f**) reached maximum of 19% at 495 nm but the longer wavelength light than 670 nm did not generate any photocurrent (Figure 3a), which is well matched with the UV-visible spectrum of **PDI-C9:P3HT** = 1:4 film. In the case of **device n**, the IPCE spectrum was also similar to absorption spectrum of **P3HT:5-PDI-DI** = 1:1 blend film, which covered the whole visible region. And the onset of IPCE spectrum was longer wavelength than 750 nm (Figure 3b) and this means the light absorbed by **5-PDI-DI** generate the photocurrent.

Thermogravimetry analysis (TGA) data of **PDIs** revealed that, **PDI-C9** is thermally stable over 400°C, but the pyrrolidinyl group

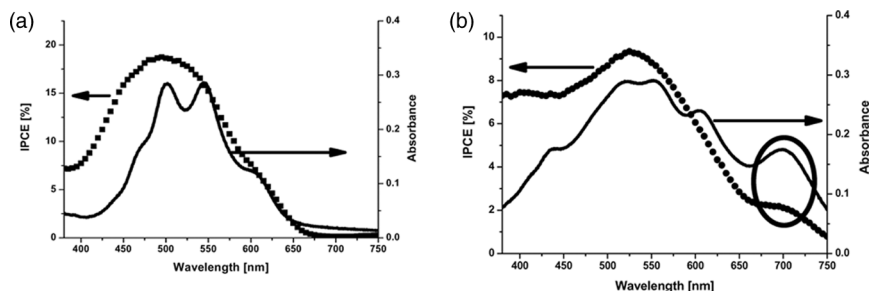


FIGURE 3 UV-visible absorption spectra of **P3HT:PDI**s blend films and incident photon-to-current conversion efficiency (IPCE) spectra of devices; a) **P3HT:PDI-C9** = 1:4 (**device f** at Table 1), b) **P3HT:5-PDI** = 1:1 (**device n**).

attached at the bay position of **5-PDI-MONO** and **5-PDI-DI** were easily decomposed even below 200°C. Our next goal is to find the other electron-donating side group that is thermally stable, because this electron-donating group will improve the V_{OC} by increasing LUMO level of perylene and possibly shifts the absorbing region to the longer wavelength and it could also act like an antenna or a wire through in which electron could transfer.

CONCLUSIONS

All of the device performances were increased by thermal annealing and the photon absorbed by PDIs converted to current. With increasing **PDI-C9** ratio in **P3HT:PDI-C9** blend system, the PCE increased gradually to get the best performance of 0.18% at 1:4 ratio. However, **5-PDI-MONO** and **5-PDI-DI** based devices showed the best performance of 0.11 and 0.18% at 1:1 blend ratio and the PCE were drastically decreased by adding more **5-PDI-MONO** and **5-PDI-DI**. The absorption spectra of PDIs were shifted to 100 nm longer wavelength region by introducing each pyrrolidinyl group. The V_{oc} of the devices were increased nearly 0.3 V by introducing two electron donating pyrrolidinyl groups from **PDI-C9** (~0.3 V) to **5-PDI-DI** (~0.6 V).

REFERENCES

- [1] (a) Padinger, F., Rittberger, R. S., & Sariciftici, N. S. (2003). *Adv. Funct. Mater.*, **13**, 85; (b) Brabec, C. J. (2004). *Sol. Energy Mater. Sol. Cells*, **83**, 273.
- [2] Neuteboom, E. E., Meskers, S. C. J., Van Hal, P. A., Van Duren, J. K. J., Meijer, E. W., Janssen, R. A. J., Dupin, H., Pourtois, G., Cornil, J., Lazzaroni, R., Bredas, J.-L., & Beljonne, D. (2003). *J. Am. Chem. Soc.*, **125**, 8625.

- [3] Boom, T., Hayes, R. T., Zhao, Y., Bushard, P. J., Weiss, E. A., & Wasielewski, M. R. (2002). *J. Am. Chem. Soc.*, *124*, 9582.
- [4] Liu, S.-G., Sui, G., Cormier, R. A., Leblanc, R. M., & Gregg, B. A. (2002). *J. Phys. Chem. B*, *106*, 1307.
- [5] (a) Ferrere, S. & Gregg, B. A. (2002). *New J. Chem.*, *26*, 1155; (b) Wang, S., Li, Y., Du, C., Shi, Z., Xiao, S., Zhu, D., Gao, E., & Cai, S. (2002). *Synthetic Metals*, *128*, 299.
- [6] (a) Nakamura, J., Yokoe, C., Mruata, K., & Takahashi, K. (2004). *J. Appl. Phys.*, *96*, 6878; (b) Bettignies, R., Nicolas, Y., Blanchard, P., Levillain, E., Nunzi, J.-M., & Roncali, J. (2003). *Adv. Mater.*, *15*, 1939; (c) Breeze, A. J., Salomon, A., Ginley, D. S., Gregg, B. A., Tillmann, T., & Horhold, H.-H. (2002). *Appl. Phys. Lett.*, *81*, 3085; (d) Kim, J. Y. & Bard, A. J. (2004). *Chemical Physics Letters*, *383*, 11.
- [7] Dittmer, J. J., Marseglia, E. A., & Friend, R. H. (2000). *Adv. Mater.*, *12*, 1270.
- [8] Zhao, Y. & Wasielewski, M. R. (1999). *Tetrahedron Lett.*, *40*, 7047.
- [9] Sirringhaus, H., Tessler, N., & Friend, R. H. (1998). *Science*, *280*, 1741.
- [10] Wescott, L. D. & Mattern, D. L. (2003). *J. Org. Chem.*, *68*, 10058.